

## Dark Matter Halos around Galaxies

P. Salucci

*SISSA, via Beirut 2-4, I-34013 Trieste, Italy*

M. Persic

*Osservatorio Astronomico di Trieste, via Beirut 2-4, I-34013 Trieste, Italy*

### Abstract.

We present evidence that all galaxies, of any Hubble type and luminosity, bear the kinematical signature of a mass component distributed differently from the luminous matter. We review and/or derive the DM halo properties of galaxies of different morphologies: spirals, LSBs, ellipticals, dwarf irregulars and dwarf spheroidals.

We show that the halo density profile

$$M_h(x) = M_h(1) (1 + a^2) \frac{x^3}{x^2 + a^2}$$

(with  $x \equiv R/R_{opt}$ ), across both the Hubble and luminosity sequences, matches all the available data that include, for ellipticals: properties of the X-ray emitting gas and the kinematics of planetary nebulae, stars, and HI disks; for spirals, LSBs and dIrr's: stellar and HI rotation curves; and, finally, for dSph's the motions of individual stars.

The dark + luminous mass structure is obtained: (a) in spirals, LSBs, and dIrr's by modelling the extraordinary properties of the Universal Rotation Curve (URC), to which all these types conform (i.e. the URC luminosity dependence and the smallness of its rms scatter and cosmic variance); (b) in ellipticals and dSph's, by modelling the coadded mass profiles (or the  $M/L$  ratios) in terms of a luminous spheroid and the above-specified dark halo.

A main feature of galactic structure is that the dark and visible matter are well mixed already in the luminous region. The transition between the inner, star-dominated regions and the outer, halo-dominated region, moves progressively inwards with decreasing luminosity, to the extent that very-low- $L$  stellar systems (disks or spheroids) are not self-gravitating, while in high- $L$  systems the dark matter becomes a main mass component only beyond the optical edge.

A halo core radius, comparable to the optical radius, is detected at all luminosities and for all morphologies. The luminous mass fraction varies with luminosity in a fashion common to all galaxy types: it is comparable with the cosmological baryon fraction at  $L > L_*$  but it decreases by more than a factor  $10^2$  at  $L \ll L_*$ .

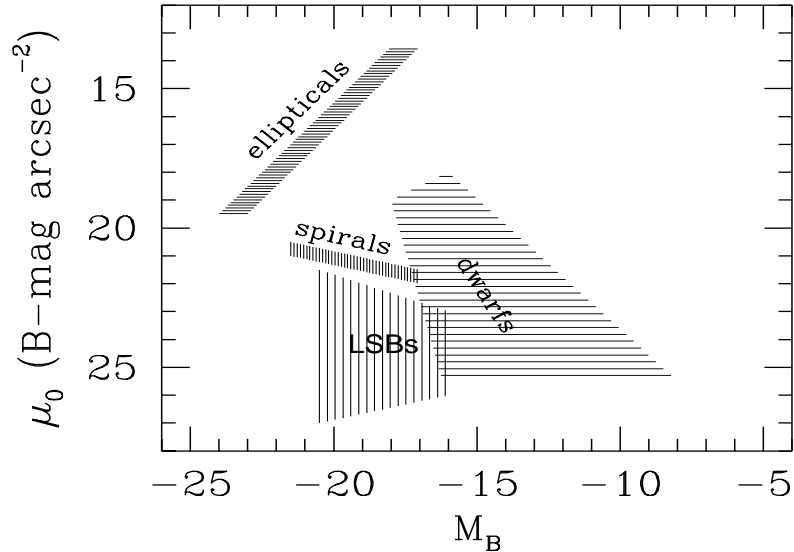


Figure 1. The loci populated by the various families of galaxies in the central brightness vs. luminosity plane.

For each Hubble type, the central halo density increases with decreasing luminosity: sequences of denser stellar systems (dwarfs, ellipticals, HSBs, LSBs in decreasing order) correspond in turn to sequences of denser halos.

Then, the dark halo structure of galaxies fits into a well ordered pattern underlying a unified picture for the mass distribution of galaxies across the Hubble sequence.

## 1. Introduction

Over scales  $\sim 1$  kpc up to the Hubble radius, the dynamics of cosmological systems is influenced, and often dominated, by non-radiating matter which reveals itself only through a gravitational interaction with the luminous matter. As the observational evidence has been accumulating, it has become apparent that understanding the nature, history and structural properties of this dark component, is the focal point of Cosmology at the end of the millennium. In particular, the halos of dark matter, detected around galaxies, have driven the dissipative infall of baryons that, modulo a variety of initial conditions, has built the bulge/disk/spheroid systems we observe today. It is remarkable that the  $\sim 10^{11}$  galaxies present within the Hubble radius can be classified in a very small number of types: ellipticals, spirals, low-surface-brightness (LSB) galaxies, dwarf spirals and dwarf irregulars. The main characterizing property of these families is their position in the  $\mu_0, M_B$  (central surface brightness, magnitude)

plane (see Fig. 1). In this plane spiral galaxies lie at the center and show a very small range ( $\sim 0.5$  mag) in  $\mu_0$ ; ellipticals are very bright systems, and span only a factor 10 in luminosity, that however well correlates with central brightness; LSB galaxies are the counterpart of spirals at low surface brightness; and, finally, dwarfs are very-low-luminosity spheroids or disks which barely join the faintest normal systems and span the largest interval in  $\mu_0$ . Cosmologically, all galaxy types are equally important for at least two reasons: (a) those types having a lower average luminosity are however much more numerous and hence can store a significant amount of baryons, and (b) the properties that characterize and differentiate the various Hubble types, i.e. the angular momentum content and the stellar populations, are intimately related to the process of galaxy formation.

A systematic presence of dark matter was first found in spirals, specifically from the non-keplerian shape of their rotation curves (Rubin et al. 1980; Bosma 1981), and in dSph's from their very high tidal  $M/L$  ratios (Faber & Lin 1983). Later, dark matter has been systematically found also around dwarf spirals and LSB galaxies (Romanishin et al. 1982). For ellipticals, the situation is less clear: certainly at least some (if not all) show evidence of a massive dark halo in which the luminous spheroid is embedded (e.g. Fabricant & Gorenstein 1983). Therefore, the claim for the ubiquitous presence of dark halos around galaxies may be observationally supported.

Theoretically, this claim is the natural outcome of the bottom-up cosmological scenarios in which galaxies form inside dark matter halos (probably with a universal density profile; e.g., Frenk et al. 1988 and Navarro et al. 1996). We point out that this prediction has so far been tested only in spirals where reliable DM profiles have been obtained (Persic, Salucci & Stel 1996; hereafter PSS96). Along the Hubble sequence, the systematic presence of dark matter in galaxies and its relation with the luminous matter has so far been poorly known. However, in the past year or so a number of observational breakthroughs (some of which presented at this conference) have allowed us to obtain the gravitational potential in numerous galaxies of different Hubble types (including also LSB galaxies).

The time is now ripe for attempting to derive the general mass profile of dark matter halos, as a function of galaxy luminosity and morphology. In this paper (which is also a review describing much recent work), we will try to answer, for the first time, a simple (cosmological) question: Given a galaxy of Hubble type  $T$  and luminosity  $L$ , which halo is it embedded in?

The aim of this article is then to derive/review, by means of proper mass modelling, the mass distribution in galaxies of different luminosities and Hubble Types and to fit all of the various pieces into one unified scheme of galaxy structure. Notice that the theoretical implications of the results presented here will be discussed elsewhere. In detail, the plan of the paper is as follows: in section 2 we review the properties of DM halos in spiral galaxies; in section 3 we work out the DM mass distribution in LSBs and perform a comparative analysis with that in spirals; in section 4 we derive/review the halo properties of elliptical galaxies; in sections 5 and 6 we derive the properties of dwarf galaxies, irregulars and spheroidals. Finally, in section 7 we propose a unified scheme for the DM halos around galaxies and their interaction with the luminous matter. (A value of  $H_0 = 75 \text{ km s}^{-1} \text{ Mpc}^{-1}$  is assumed throughout.)

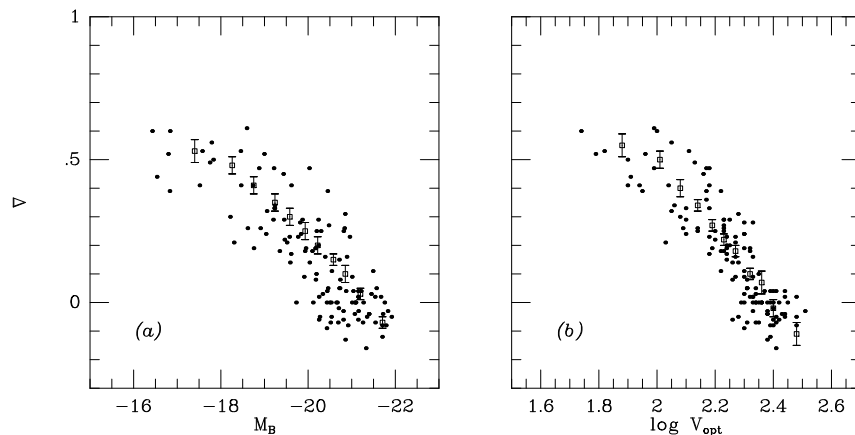


Figure 2. The RC slope at  $R_{opt}$  vs luminosity (*left*) and  $V_{opt}$  (*right*) for the 1100 RCs of Persic & Salucci 1995 and PSS96.

## 2. Spiral Galaxies

The luminous ( $\sim$ stellar) matter in spiral galaxies is distributed in two components: a concentrated, spheroidal bulge, with projected density distribution approximately described by

$$I(R) = I_0 e^{-7.67 (R/r_e)^{1/4}} \quad (1)$$

(with  $r_e$  being the half-light radius; but see Broeils & Courteau 1997), and an extended thin disk with surface luminosity distribution very well described (see Fig.3) by:

$$I(R) = I_0 e^{-R/R_D} \quad (2)$$

(with  $R_D$  being the disk scale-length; Freeman 1970). Let us take  $R_{opt}$  as the radius encircling 83% of the integrated light: for an exponential disk  $R_{opt} = 3.2 R_D$  is the limit of the stellar disk. The relative importance of the two luminous components defines the Hubble sequence of spirals, going from the bulge-dominated Sa galaxies to the progressively more disk-dominated Sb/Sc/Sd galaxies. We recall that the spiral arms are non-axisymmetric density perturbations, traced by newly-formed bright stars or HII regions, which are conspicuous in the light distribution and perturb the circular velocity field through small-amplitude sinusoidal disturbances (i.e., wiggles in the rotation curves), but they are immaterial to the axisymmetric gravitational potential. This digression is to recall that fitting these features with a mass model is a mistake!

The rotation curves of spiral galaxies do not show any keplerian fall-off at outer radii (e.g.: Rubin et al. 1980; Bosma 1981). Moreover, their shapes at  $R > (1 - 2)R_D$  are inconsistent with the light distribution, so unveiling the presence of a DM component. PSS96, analyzing approximately 1100 RCs, about 100 of which extended out to  $\lesssim 2 R_{opt}$ , found that the luminosity specifies the entire axisymmetric rotation field of spiral galaxies. At any chosen normalized

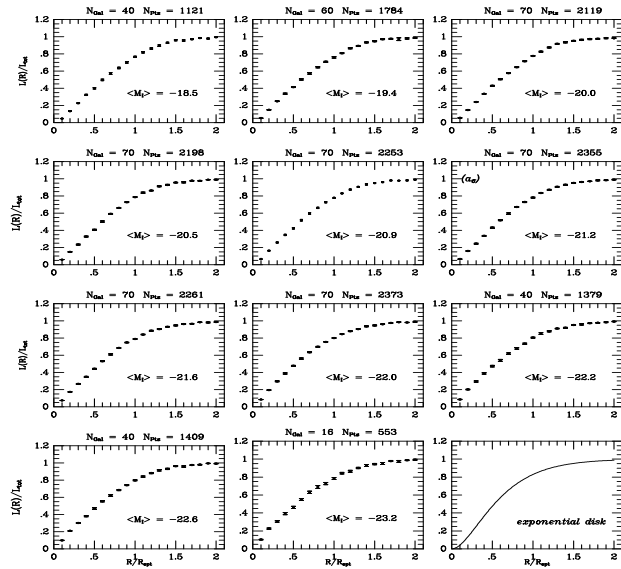


Figure 3. Averaged spirals  $I$ -light profiles at different luminosities. Each  $L$  bin includes hundredths of galaxies

radius  $x \equiv R/R_{opt}$ , both the RC amplitude and the local slope strongly correlate with the galaxy luminosity (in particular, for  $x = 1$  see Fig. 2; for outer radii see PSS96, Salucci & Frenk 1989, and Casertano & van Gorkom 1991). Remarkably, the rms scatter around such relationships is much smaller than the variation of slopes among galaxies (see PSS96). This has led to the concept of the *Universal Rotation Curve* (URC) of spiral galaxies (PSS96 and Persic & Salucci 1991; see Fig.5). The rotation velocity of a galaxy of luminosity  $L/L_*$  at a radius  $x \equiv R/R_{opt}$  is well described by:

$$\begin{aligned}
 V_{URC}(x) = & V(R_{opt}) \left[ \left( 0.72 + 0.44 \log \frac{L}{L_*} \right) \frac{1.97 x^{1.22}}{(x^2 + 0.78^2)^{1.43}} + \right. \\
 & \left. + \left( 0.28 - 0.44 \log \frac{L}{L_*} \right) \left[ 1 + 2.25 \left( \frac{L}{L_*} \right)^{0.4} \right] \frac{x^2}{x^2 + 2.25 \left( \frac{L}{L_*} \right)^{0.4}} \right]^{1/2} \text{ km s}^{-1}.
 \end{aligned}
 \tag{3}$$

(with  $\log L_*/L_\odot = 10.4$  in the  $B$ -band). Remarkably, spirals show a very small cosmic variance around the URC. In 80% of the cases the difference between the individual RCs and the URC is smaller than the observational errors, and in most of the remaining cases it is due to a bulge not considered in eq.(3) (Hendry et al. 1997; PSS96). This result has been confirmed by a Principal Component Analysis study of URC (Rhee 1996; Rhee & van Albada 1997): they found that the two first components alone account for  $\sim 90\%$  of the total variance of the RC shapes. Thus, spirals sweep a narrow locus in the RC-profile/amplitude/luminosity space.

The luminosity dependence of the URC strongly contrasts with the self-similarity of the luminosity distribution of stellar disks (Fig. 3): the luminosity profiles  $L(x) \propto \int_0^x x I(x) dx$  do not depend on luminosity. This reflects the

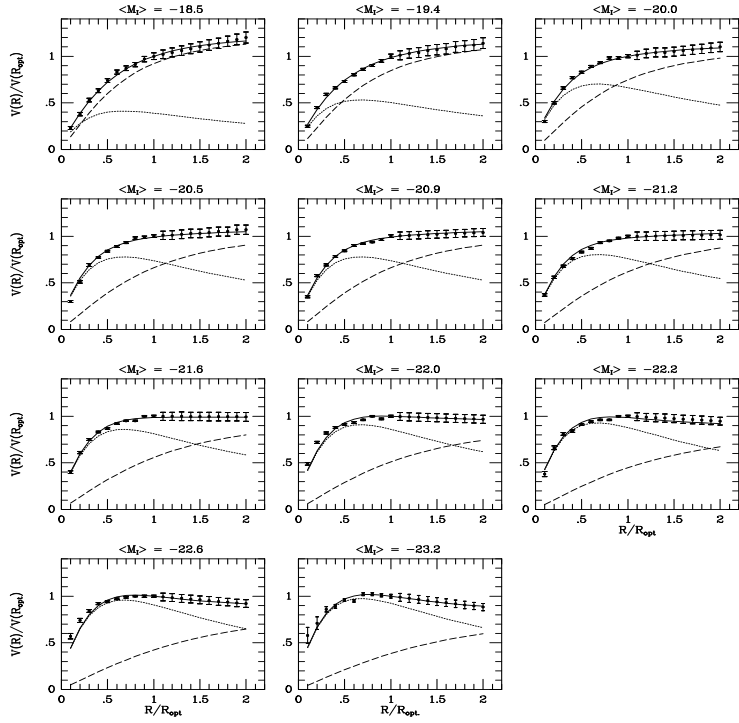


Figure 4. Coadded rotation curves (filled circles with error bars) reproduced by URC (solid line) Also shown the separate dark/luminous contributions (dotted line: disk; dashed line: halo.)

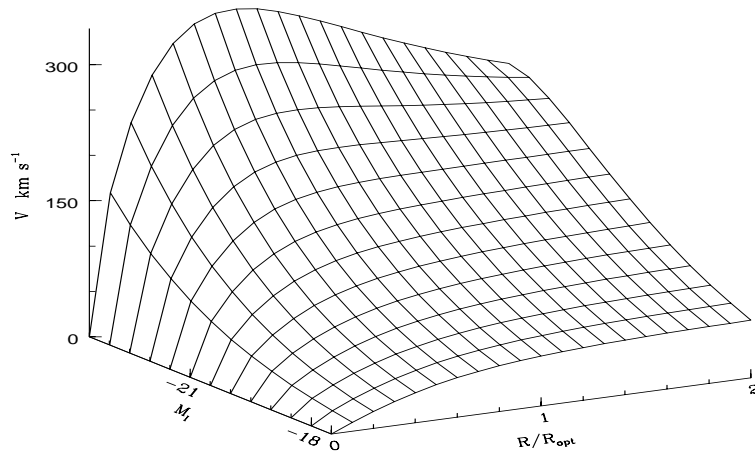


Figure 5. The URC surface.

discrepancy between the distribution of light and that of the gravitating mass. Noticeably, this discrepancy increases with radius  $x$  and with decreasing galaxy luminosity  $L$ . The URC can be fitted by a combination of two components: (a) an exponential thin disk, approximated for  $0.04R_{opt} < R \leq 2R_{opt}$  as

$$V_d^2(x) = V^2(R_{opt}) \beta \frac{1.97 x^{1.22}}{(x^2 + 0.78^2)^{1.43}}, \quad (4)$$

and (b) a spherical halo represented by

$$V_h^2(x) = V^2(R_{opt}) (1 - \beta) (1 + a^2) \frac{x^2}{(x^2 + a^2)}, \quad (5)$$

$$M_h(x) = G^{-1} V^2(1) R_{opt} (1 - \beta) (1 + a^2) \frac{x^3}{(x^2 + a^2)},$$

with  $x \equiv R/R_{opt}$  being the normalized galactocentric radius,  $\beta \equiv V_d^2(R_{opt})/V_{opt}^2$  the disk mass fraction at  $R_{opt}$ , and  $a$  the halo core radius (in units of  $R_{opt}$ ). The disk+halo fits to the URC are extremely good (fitting errors are within 1% on average) at all luminosities (see Fig. 4) when

$$\beta = 0.72 + 0.44 \log\left(\frac{L}{L_*}\right), \quad (6)$$

$$a = 1.5 \left(\frac{L}{L_*}\right)^{1/5}. \quad (7)$$

Thus we detect, for the DM component, a central constant-density region of size  $\sim R_{opt}$ , slightly increasing with luminosity. The transition between the inner, luminous-matter-dominated regime and the outer, DM-dominated regime occurs well inside the optical radius: typically at  $r \ll R_{opt}$  in low-luminosity galaxies, and farther out, closer to  $\sim R_{opt}$ , at high luminosities (see Fig.4). Thus, the ordinary and dark matter are well mixed in the very stellar regions of spirals.

The total halo mass can be evaluated by extrapolating the halo out to the radius,  $R_{200}$ , encompassing a mean overdensity of 200. We find:

$$R_{200} = 250 \left(\frac{L}{L_*}\right)^{0.2} \text{ kpc} \quad (8)$$

$$M_{200} \sim 2 \times 10^{12} \left(\frac{L}{L_*}\right)^{0.5} M_{\odot}, \quad (9)$$

in good agreement with results derived from satellite and pair kinematics (Charlton & Salpeter 1991; Zaritsky et al. 1993). Notice that

$$\frac{M_{200}}{L_B} \simeq 75 \left(\frac{L_B}{L_*}\right)^{-0.5} \quad (10)$$

(in solar units). This implies that the halo mass function is not parallel to the observed galaxy luminosity function (Ashman, Salucci & Persic 1993).

The luminosity dependence of the disk mass fraction can be interpreted in terms of a mass-dependent efficiency in transforming the primordial gas fraction into stars. In fact, the total (i.e., computed at  $R_{200}$ ) luminous mass fraction of a galaxy of luminosity  $L$  is:

$$\frac{M_{\star}}{M_{200}} \simeq 0.05 \left( \frac{L}{L_{\star}} \right)^{0.8}. \quad (11)$$

This suggests that only the brightest objects reach a value comparable with the primordial value  $\Omega_{BBN} \lesssim 0.10$ , while in low- $L$  galaxies only a small fraction of their original baryon content has been turned into stars. The luminosity dependence of the DM fraction found by Persic & Salucci (1988, 1990) has been confirmed by direct mass modelling (e.g.: Broeils 1992; Broeils & Courteau 1997; Sincotte & Carignan 1997; see also Ashman 1992).

On scales  $(0.2 - 1) R_{200}$ , the halos have mostly the same structure, with a density profile very similar at all masses and an amplitude that scales only very weakly with mass, like  $V_{200} \propto M_{200}^{0.15}$ . This explains why the kinematics of satellite galaxies orbiting around spirals show velocities (relative to the primary) uncorrelated with the primary's luminosity (Zaritsky 1997). At very inner radii, however, the self-similarity of the profile breaks down, the core radius becoming smaller for decreasing  $M_{200}$  according to:

$$\frac{\text{core radius}}{R_{200}} = 0.075 \left( \frac{M_{200}}{10^{12} M_{\odot}} \right)^{0.6}. \quad (12)$$

The central density scales with mass as:

$$\rho_h(0) = 6.3 \times 10^4 \rho_c \left( \frac{M_{200}}{10^{12} M_{\odot}} \right)^{-1.3} \quad (13)$$

( $\rho_c$  is the critical density of the universe).

The regularities of the luminous-to-dark mass structure can be represented as a curve in the space defined by dark-to-luminous mass ratio, (halo core radius)-to-(optical radius) ratio, central halo density (see PSS96). This curve is a structural counterpart of the URC and represents the only locus of the manifold where spiral galaxies can be found. The main properties of dark matter in spiral galaxies can then be summarized as follows:

- substantial amounts of dark matter are detected in the optical regions of all spirals, starting at smaller radii for lower luminosities;
- the dark and the luminous matter are well mixed;
- the structure of the halos is universal: it involves a core radius comparable in size with the optical radius and a central density scaling inversely with luminosity;
- the ratio between luminous and dark matter is a function of luminosity (or mass) among galaxies. At a given (normalized) radius, this ratio increases with increasing luminosity: the global visible-to-dark mass ratio spans the range between  $\sim \Omega_{BBN}$  at very high luminosities and  $\sim 10^{-4}$  at  $L \ll L_{\star}$ .

The discovery of these features, describing the various stages of the processes leading to present-day galaxies, supersedes the observationally disproved paradigms of "flat rotation curves" and "cosmic conspiracy".



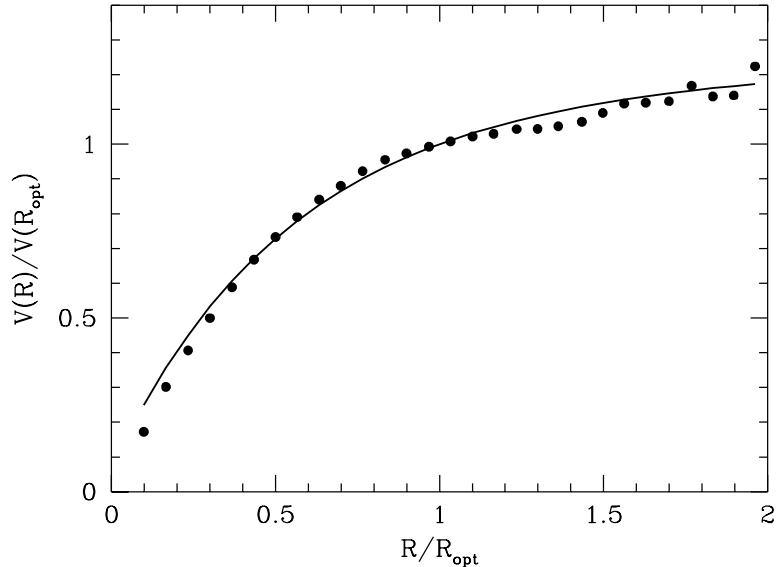


Figure 6. Coadded rotation curve of the sample of LSB galaxies with  $V_{opt} \sim (70 \pm 30) \text{ km s}^{-1}$ . The solid line represents the  $V_{URC}$  of spirals of similar  $V_{opt}$ .

### 3. Low-Surface-Brightness Galaxies

The central surface luminosity of spirals is normally about constant, at  $\mu_0(B) = 21.65 \pm 0.30$ . Recently, however, a large population of disk systems with a significantly lower surface brightness ( $\mu_0(B) = 24 - 25$ ) has been detected (Schombert et al. 1992; Driver et al. 1994; Morshidi et al. 1997; see also Disney & Phillips 1983). In these systems the light distribution follows that of an exponential thin disk (McGough & Bothun 1994), with total magnitude  $\sim 1.5$  mag fainter than that of normal (HSB) spirals. At the faint end of the LSB luminosity distribution ( $M_B \sim -16$ ), the galaxies have very extended HI disks whose kinematics yields the mass structure (de Blok, McGaugh & van der Hulst 1996). In detail, de Blok et al. have published the HI rotation curves of 19 low- $L$  LSBs, having  $M_B \sim -17$  mag,  $V_{max} \sim 70 \text{ km s}^{-1}$ , and (remarkably)  $R_{opt} \sim (8 - 10) \text{ kpc}$ , roughly independent of luminosity. These galaxies are the counterpart of the faintest HSB spirals. Notice that, although the maximum velocities are similar, the optical sizes of LSBs are  $\sim 3$  times larger than those of HSBs.

The objects in de Blok et al. (1996) are all within a small range of magnitudes and optical velocities,  $M_B = -17 \pm 0.5$ ,  $V_{opt} \sim (70 \pm 30) \text{ km s}^{-1}$ . From these data we construct, as we did for spirals, the coadded rotation curve  $V(\frac{R}{R_{opt}}, 70)$ . Notice that, unlike for spirals, rotation curves of LSBs with higher  $V_{opt}$  are not available: so we can compare LSB and spiral RCs only at their lowest velocities, shown for spirals in the top left panel in Fig.4 and for LSBs in Fig.6 (points). In detail, in the latter figure we plot  $V(R/R_{opt})$ , the coadded RC obtained from the de Blok et al. data, together with the spiral  $V_{URC}$  for the same range of maximum velocities (50–100  $\text{km s}^{-1}$ ) (see PSS96 for all of the details). The

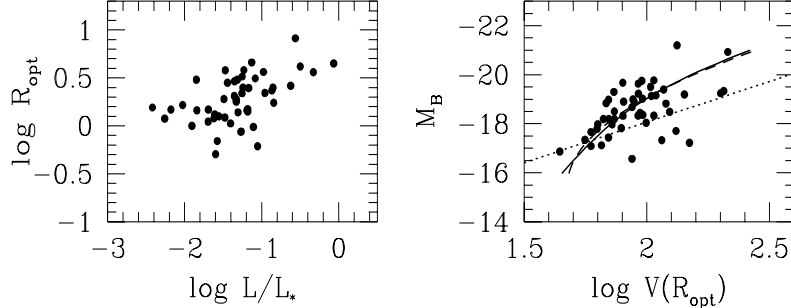


Figure 7. The radius–luminosity relation (*left*) and the Tully-Fisher relation (*right*) for the Matthews sample of LSBs. Dashed curve: fit to the data. Solid curve: predictions of a mass model identical to that of spirals. Dotted line: prediction of a mass model model with constant ( $M/L$ )

agreement is striking: no difference can be detected between the LSB and HSB rotation curves, which coincide within the observational uncertainties. Notice that the LSB and HSB rotation curves are identical when the radial coordinate is normalized to the disk length-scale (essential procedure for determining the DM distribution). The fact that, when expressed in physical radii, LSB rotation curves rise to their maximum more gently than HSB RCs (see Fig.3 of de Blok & McGough 1997), depends exclusively on the larger LSB disk scalelengths.

For LSBs we adopt a mass model including, as for spirals, (*i*) an exponential thin disk and (*ii*) a dark halo of mass profile given by eq.(5). The LSB coadded RC is extremely well fitted by eqs.(4) and (5) with the ‘spiral’ values  $\beta = 0.1 \pm 0.04$  and  $a \simeq 0.75$ . These parameters imply that LSB galaxies are completely dominated by a dark halo with a large  $\sim (5 - 6)$  kpc core radius.

Higher-luminosity (up to  $M_B \sim -22$ ) LSBs do exist (e.g., Sprayberry et al. 1993): their structure can be tentatively investigated by means of their Tully-Fisher relationship. Observationally, these objects show a good correlation between luminosity and the corrected linewidth  $w_{0,i}$  (Matthews et al. 1997):

$$\log w_{0,i} = 2.41 + 0.69 \log\left(\frac{L_V}{L_V^*}\right) + 0.16 \log^2\left(\frac{L_V}{L_V^*}\right), \quad (14)$$

where  $L_V^*$  corresponds to  $M_V^* = -20.87$  (see Fig. 7). The quantity  $w_{0,i}$  is, as in spirals, a good measure of the circular velocity at  $\sim R_{opt}$ : then

$$w_{0,i}^2 R_{opt} \simeq G [M_h(R_{opt}) + M_{bar}(R_{opt})], \quad (15)$$

where  $M_{bar} = M_D + M_{HI}$ . For LSB spirals we take the same dark-to-visible mass ratios as for HSB spirals,  $\frac{M_h(R_{opt})}{M_{bar}(R_{opt})} \simeq 9 \times \left(\frac{L_B}{0.04 L_*}\right)^{-1}$  (see conclusions of PSS96), and we assume  $M_{bar}(R_{opt}) \propto L_B^k$ . Finally, by using the LSB luminosity-radius relation,  $R_{opt} = 12 (L/L_*)^{0.25}$  kpc (see Fig. 7), we are able to reproduce

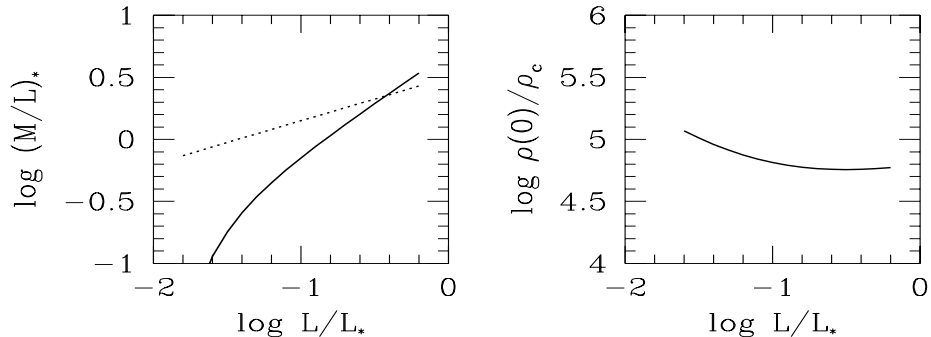


Figure 8. LSB  $(M/L)_*$  (left: solid curve; the dotted line refers to spirals) and central overdensity (right) as a function of luminosity.

the observed  $M_V$ - $\log w_{0,i}$  relation: in Fig. 7 we show the excellent agreement between the observed linewidths and those predicted by our mass model when  $k = 1.8$  and the LSBs stay on the ‘spiral’  $\beta$ - $L$  and  $a$ - $L$  relationships.

At  $\sim L_*$ , the LSB stellar  $M/L$  ratios are similar to those of HSBs, but they decline steeply with decreasing luminosity (see Fig. 8, left panel). This result is in good agreement with the  $(M/L)_*$  ratios obtained by applying the maximum-disk hypothesis to solve for the galactic structure: in this case  $\log(M/L)_*$  increases from  $\sim -0.3$  to  $0.5$  across the entire LSB luminosity (velocity) range (de Blok & McGaugh 1997).

The central overdensities,  $3/(4\pi G\rho_c)(1-\beta)(V_{opt}/R_{opt})^2(1+a^2)/a^2$ , are shown in Fig. 8 (right panel) as a function of luminosity. They are smaller and less dependent on galaxy luminosity than those in normal spirals, in agreement with the findings by de Blok & McGaugh (1997).

With the caveat of the relative smallness of the present sample, we claim that LSB galaxies are indistinguishable from HSBs in the  $(\beta, a)$  space describing the coupling between dark and visible matter.

To end this section, we comment on the argument, raised sometimes, according to which the discovery of a large number of LSBs would make the findings on DM in spirals (e.g. PSS96) irrelevant, in that normal spirals would represent an unfair, biased sample of galaxies. There is no doubt that the existence of a population of LSB galaxies, contiguous to the HSBs, affects the interpretation, and even the physical meanings, of luminosity functions and number counts. However, it is exactly the characteristic difference between the two families that answers the point. Even prior to any mass modelling, we can argue that in the Universe there are about  $10^{11}$  disk systems obeying the ‘Freeman law’:  $\mu_0 = 21.5 \pm 0.5$  independent of galaxy luminosity. It is obviously necessary to know the DM properties of this family, independently of the existence of another family of disk systems not obeying such a ‘law’, and maybe not even observable. Of course, investigating the DM properties of LSBs is equally important and crucial. Furthermore, the argument raised above appears even more immaterial after the analysis of the LSB rotation curves. In fact, as far as the structural parameters are concerned, HSBs and LSBs are indistinguishable. In

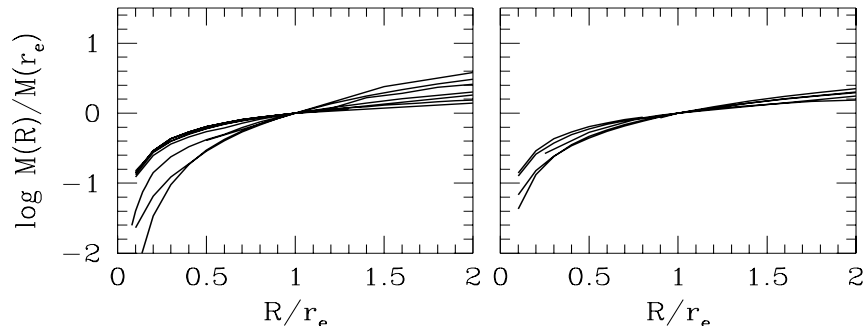


Figure 9. The mass as a function of radius for the ellipticals of our subsamples, with luminosities  $\langle \log L/L_* \rangle = -0.4$  and  $\langle \log L/L_* \rangle = 0.4$  (left and right, respectively).

other words, LSBs follow the spiral  $V_{\text{URC}}(R/R_{\text{opt}})$ , but strongly deviate with respect to the spirals' luminosity–(disk length-scale) relation.

#### 4. Elliptical Galaxies

Elliptical galaxies are pressure-supported, triaxial stellar systems whose orbital structure may depend on their angular momentum content, degrees of triaxiality and velocity dispersion anisotropy. As is well known, the derivation of the mass distribution from stellar motions is not straightforward as it is from rotation curves in disk systems, because the kinematics of the former is strongly affected by geometry, rotation, and anisotropies. However, in addition to stellar kinematics, there are a number of mass tracers (X-ray emitting halos, planetary nebulae, ionized and neutral disks) which crucially help to probe the gravitational potential out to external radii (see Danziger 1997).

The luminosity profile  $\rho_*(r)$  of E's is obtained from the observed projected surface density, which follows the de Vaucouleurs profile [see eq.(1)], by assuming an intrinsic shape and deprojecting. A very good approximation for  $\rho_*(r)$  is the Hernquist profile:

$$\rho_*(r) = \frac{M_*}{2\pi} \frac{1}{y(y+c)^3} \quad (16)$$

(where  $y = 1.81 r/r_e$  and  $c = 1$ ). As the Hernquist profile is no longer a good fit for  $R \gg r_e$ , from actual surface-photometry profiles we have evaluated that  $R_{\text{opt}} \simeq 2r_e$ , where  $r_e = 6(L/L_*)^{0.7}$  kpc (from Djorgovski & Davis 1987). All ellipticals belong, within a very small cosmic scatter ( $< 12\%$ ), to a relation of the type:

$$r_e \propto \sigma_0^A I_e^B, \quad (17)$$

where  $r_e$  is the half-light radius,  $I_e$  is the mean surface brightness within  $r_e$ , and  $\sigma_0$  is the observed (projected) central velocity dispersion. In the logarithmic space, this corresponds to a plane, the Fundamental Plane of ellipticals (Djor-

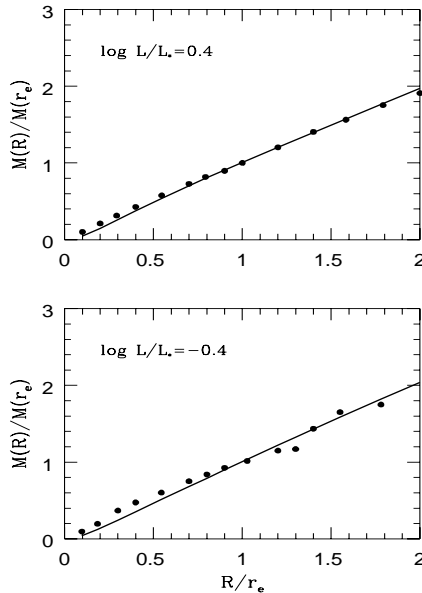


Figure 10. Coadded mass profile of ellipticals, filled circles, with the best fit mass model (solid line)

govski & Davis 1987; Dressler et al. 1987), that constrains the properties of the DM distribution.

Observations indicate  $A = 1.23$  (1.66) and  $B = -0.82$  ( $-0.75$ ) in the  $V$ -band and  $K$ -band, respectively (e.g., Djorgovski & Santiago 1993). Assuming a constant  $M/L$  and structural homology, the virial theorem predicts  $A = 2$ ,  $B = -1$ . The simplest explanation of the departure of  $A$  from the virial expectation involves a systematic variation of  $M/L$  with  $L$ , which also accounts for the wavelength dependence of  $A$  (Djorgovski & Santiago 1993). The departure of  $B$  from the virial expectation is likely to be due to the breakdown of the homology of the luminosity structure (see Caon, Capaccioli & D’Onofrio 1993; Graham & Colless 1997). Assuming spherical symmetry and isotropic stellar motions (so  $M_\star \simeq 3.4G^{-1}\sigma_0^2 r_e$  and  $L = 2\pi I_e r_e^2$ ), the FP implies that  $M/L|_{r_e}$ , inclusive of dark matter, is “low”: 4–9 (Lanzoni 1994; Bender, Burstein & Faber 1992), and roughly consistent with the values predicted by the stellar population models (Tinsley 1981). No large amounts of DM are needed on these scales, as it also emerges from mass models of individual ellipticals, obtained by analyzing the line profiles of the l.o.s velocity dispersion (van der Marel & Franx 1993), which show that the DM fraction inside  $r_e$  is substantially less than 50% (i.e.  $M/L_B \lesssim 10$ ; see van der Marel 1991, 1994; Rix et al. 1997; Saglia et al. 1997a,b; Carollo & Danziger 1994; Carollo et al. 1995), as in spirals.

We now investigate in some detail the effects of DM on the Fundamental Plane. For this purpose, let us describe, for mathematical simplicity, the dark halo by a Hernquist profile [eq.(16)] with a lower mass concentration than the luminous spheroid:  $c = 2$  (see Lanzoni 1994). We recall that dark halos are likely to have an innermost constant-density region not described by eq.(16): this,

however, has no great relevance here, in that most of the dark mass is located outside the core where eq.(16) is likely to hold. Without loss of generality, we consider isotropic models (Lanzoni 1994): the radial dispersion velocity  $\sigma_r$  is related, through the Jeans equation, to the mass distribution by:

$$\sigma_r^2(r) = G \frac{M_{dark}(r) + M_*(r)}{r} \left( \frac{d \log \rho_*}{d \log r} \right)^{-1}. \quad (18)$$

The projected velocity dispersion is then  $\sigma_P(R) = \frac{2}{\Sigma_*(R)} \int_R^\infty \frac{\rho_*(r) \sigma_r^2(r)}{\sqrt{r^2 - R^2}} dr$ . This equation shows that, at any radius (including  $r = 0$ ), the measured projected velocity dispersion  $\sigma_P(R)$  depends on the distributions of both dark and luminous matter out to  $r \sim (2 - 3) r_e$ . Conversely, in spirals the circular velocity  $V(R)$  depends essentially only on the mass inside  $R$ , namely on just the luminous mass when  $R \rightarrow 0$ . If  $M_{200}$  is the total galaxy mass, we get

$$\sigma_P(0) = 3.4 \frac{GM_*}{r_e} \left( \frac{M_{200}}{10 M_*} \right)^{2/5}. \quad (19)$$

The mass dependence of  $\sigma_P(0)$ , combined with the thinness of the FP (i.e.:  $\delta R_e / R_e \lesssim 0.12$ ), constrains the scatter that would arise, according to eq.(19), from random variations of the total amount of DM mass in galaxies with the same luminous mass. From eq.(17) we get  $\delta \sigma / \sigma \lesssim \frac{0.12}{1.4}$ , while eq.(19) implies  $d\sigma / \sigma = 5/2 \delta M / M$ . This means that, over 2 orders of magnitude in  $M_*$ , any random variation of the dark mass must be less than 20% (Lanzoni 1994; Renzini & Ciotti 1993; Djorgovski & Davis 1987). From eq.(17) and since  $M_* \propto L^{1.2}$ , we finally get  $\frac{M_*}{M_{200}} \propto \sigma^{5/2}$ , so that  $M_{200} \propto L^{0.5-0.6}$ , as in spirals (PSS96). Let us notice that the these well-established constraints on the amount of dark matter in ellipticals, due to the existence of the Fundamental Plane, are however at strong variance with the extremely high values of the central  $M/L$  ratios, 15 – 30, found in some objects, as a result of the dynamical models of Bertin et al. (1992) and Danziger (1997).

We can determine the parameters of the dark and visible matter distribution by means of a variety of tracers of the ellipticals' gravitational field (see the review by Danziger 1997). This provides the (dark + luminous) mass distribution for 12 galaxies, with magnitudes ranging between  $-20 < M_B < -23$ . In order to investigate the luminosity dependence of the mass distribution, we divide the sample into 2 subsamples, with average values  $< \log L/L_* > = -0.4$  and  $< \log L/L_* > = 0.4$  respectively. In Fig. 9 we plot, as a function of  $R/r_e$ , the normalized mass profile of ellipticals,  $M(R)/M(r_e)$ , for each galaxy; and in Fig. 10 the coadded mass distributions for the high- $L$  and the low- $L$  subsamples that can be very well reproduced (solid lines) by a two-component mass model which includes a luminous Hernquist spheroid and a DM halo given by eq.(5). The resulting fit is excellent (see Fig.10) when  $\beta$ , the luminous mass fraction inside  $R_{opt} \simeq 2 r_e$ , scales with luminosity as in disk systems, and the halo core radius  $a$  (expressed in units of  $R_{opt}$ ) scales as

$$a = 0.8 \left( \frac{L}{L_*} \right)^{0.15}. \quad (20)$$

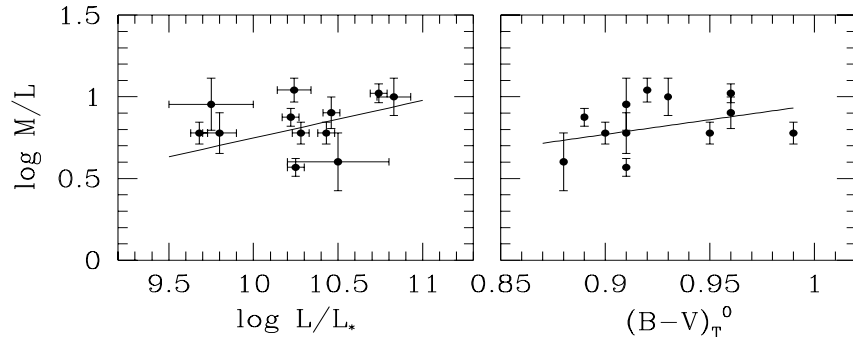


Figure 11. The  $M/L$  ratio for a sample of ellipticals as a function of luminosity (left) and color (right). The solid lines indicate the slopes of 0.2 and 1.8 (left and right, respectively).

The central density of the DM halo,  $\rho(0) \simeq 1.5 \times 10^{-3}(1 - \beta) M(R_{opt})/R_{opt}^3 (1 + a^2)/a^2$ , is 3 – 5 times larger than the corresponding densities in spirals, and it scales with luminosity in a similar way to the case of spirals. These results confirm those of the pioneering work of Bertola et al. (1993).

Finally, in Fig. 11, we show the derived  $(M/L)_*$  as a function of color (right) and of luminosity (left). The stellar mass-to-light ratios are consistent with the predictions of population synthesis models (e.g., Tinsley 1981) and are compatible with (a) the  $M/L \propto L^{0.2}$  relation deduced from the tilt of the Fundamental Plane (e.g. Diorgovski & Santiago 1993), and (b) with van der Marel’s (1991) result  $(M/L)_* \propto L^{0.35 \pm 0.05}$  (in the  $R$ -band), the only work to-date in which a dynamical derivation of stellar  $M/L$  ratios has been obtained for a large sample of ellipticals.

## 5. Dwarf Irregulars

The stellar component of these disk systems is distributed according to an exponential thin disk as in spirals (Carignan & Freeman 1988). At high luminosities, dIrr’s barely join the low- $L$  tail of spirals; at low luminosities, they reach down to  $\sim 10^{-3}L_*$ . dIrr’s have very extended HI disks: high-quality RCs can be then measured out to  $2R_{opt}$  (e.g. Côté et al. 1997; Swaters 1997). The dark matter presence is apparent when we plot (see Fig. 12) the inner and outer RC gradients,  $\nabla$  and  $\delta$ , as functions of velocity. Immediately, we realize that the DM fraction is overwhelming:  $\nabla \gg -0.3$ , gently continuing, at smaller  $V_{opt}$ , the trend of low-luminosity spirals. The extent and the quality of these RCs permit reliable determinations of the halo parameters by working out the mass model that best reproduces the RC shapes, described by the quantities  $\nabla$  and  $\delta$ .

Such a mass model includes a disk, and a dark halo with ‘spiral’ mass profile [see eq.(5)]. We recall that  $x \equiv R/R_{opt}$ ,  $a$  is the halo core radius in units of  $R_{opt}$ , and  $\beta$  is the visible mass fraction, also inclusive of the gas content, at  $x = 1$ . The outer slope  $\delta \equiv V(2)/V(1) - 1$  is related to the dark and visible matter

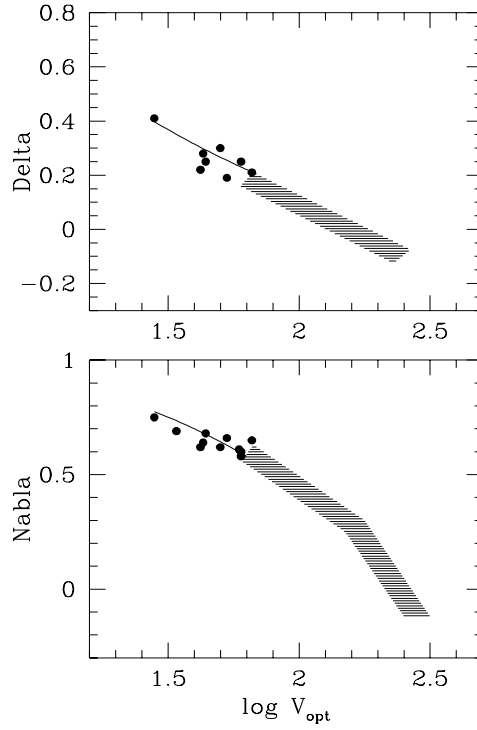


Figure 12. Inner and outer RC gradients for a sample of dIrr's from the literature. The shaded areas represent the loci populated by spirals. The solid lines are the prediction from the 'spiral' mass model.

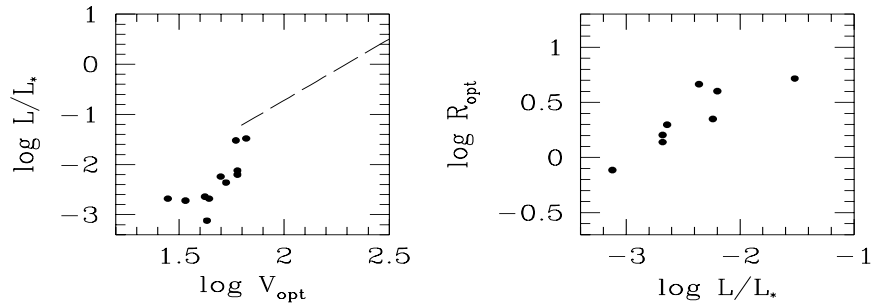


Figure 13. *Left*: the TF relation for dIrr's; the dashed line indicates the spirals TF (from PSS96). *Right*: the luminosity–radius relation for dIrr's.



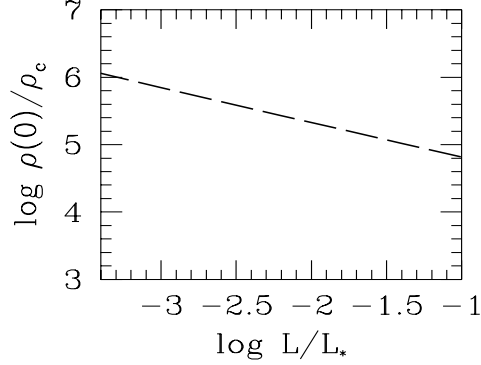


Figure 14. dIrr halo central density as a function of luminosity.

structural parameters by (see PSS96):

$$\delta = \left[ (1 + \delta_*)^2 \beta + (1 - \beta) \frac{4(1 + a^2)}{4 + a^2} - 1 \right]^{1/2}, \quad (21)$$

while the inner slope  $\nabla$  is related by

$$\nabla = \beta \nabla_* + (1 - \beta) \nabla_h, \quad (22)$$

with  $\nabla_* \sim -0.2$  including also the HI content. In detail, we aim to reproduce both the  $\nabla$ - $\log V_{opt}$  and  $\delta$ - $\log V_{opt}$  relationships, by means of the above-described mass model [from the definition:  $\nabla_h = \frac{a^2}{(1+a^2)}(0.86+0.5/a)$ ]. The contribution of the baryonic disk (stars + gas) to the circular velocity is roughly constant with radius (e.g., Carignan & Freeman 1988): the decrease of the stellar contribution outside  $R_{opt} = 5 \times (\frac{L}{0.04 L_*})^{0.45}$  is counterbalanced by the increase of the gas contribution, and therefore  $\delta_* \simeq 0$ . An excellent agreement between the model and observations is reached when:

$$a = 0.93 \times \left( \frac{V_{opt}}{63 \text{ km s}^{-1}} \right)^{-0.5}, \quad (23)$$

and

$$\beta = 0.08 \times \left( \frac{V_{opt}}{63 \text{ km s}^{-1}} \right)^{1.2}. \quad (24)$$

A luminosity-velocity relation for dIrr's, shown in Fig. 13, continues down to  $M_B = -14$  the TF relationship for spirals, allowing us to write the halo structural parameters as a function of galaxy luminosity:

$$V_{opt} = 63 \left( \frac{L}{0.04 L_*} \right)^{0.16} \text{ km s}^{-1} \quad (25)$$

The central DM density computed by means of eqs.(24), (5), (23), is plotted in Fig. 14. We realize that dwarf galaxies have the densest halos, continuing the

inverse trend with luminosity of spirals. Finally, these objects are the darkest in the Universe:  $\beta$  continues to decrease at lower luminosities down to  $\sim 10^{-2}$ . Notice that dIrr halos may have “larger” core radii, in units of  $R_{opt}$ , inverting the trend with luminosity detected in larger objects.

These results are in good agreement with the best-fit mass models of individual RCs (Puche & Carignan 1991; Broeils 1992; Côté et al. 1997; Swaters 1997). They in fact show that DM halos, with large core radii  $> R_D$ , completely dominate the mass distribution of these objects. In greater detail, Côté (1995) and Côté et al. (1997) compiling previous work find that, at  $x \simeq 2$ ,  $M_{dark}/M_{bar} = 1 - (M_B + 20)$  and that central densities increase by a factor  $\sim 10$  from  $M_B = -20$  and  $M_B = -14$ . Both results are in good agreement with the present work.

Let us point out that dIrr’s, although having a negligible amount of light, do have quite a large mass:  $\sim 8 \times 10^{10} (L/L_{max})^{1/3}$  with  $L_{max} = 0.04 L_*$  being the maximum luminosity observed in this family.

## 6. Dwarf Spheroidals

Dwarf ellipticals/spheroidals (dSph’s) are the faintest observed galaxies in the Universe and the least luminous stellar systems. Yet they represent the most common type of galaxy in the nearby universe (e.g., Ferguson & Binggeli 1994).

Given the low surface brightnesses involved, the main kinematical quantity tracing the gravitational potential, i.e. the velocity dispersion, can be determined by measuring redshifts of individual stars. Ever since early measurements of dSph velocity dispersions, high  $M/L$  ratios were derived implying large amounts of DM in these objects (Faber & Lin 1983). Kormendy (1988) and Pryor (1992) have shown that dSph’s are DM dominated at all radii: core fitting methods (Richstone & Tremaine 1986) yielded central DM densities of  $0.1 M_\odot \text{pc}^{-3}$  (i.e., overdensities of  $10^7$ ), a factor 10–100 larger than the stellar ones.

However, only recent kinematic studies (Armandroff et al. 1995; Hargreaves et al. 1994, 1996; Ibata et al. 1997; Mateo 1994; Quéroz et al. 1995; Vogt et al. 1995) have gathered a suitable number ( $\gtrsim 10$ ) of galaxies with central velocity dispersion derived by repeat measurements of motions of  $\gg 10$  stars. Mateo (1997), analysing this observational data, has shown that the central  $M/L$  increases with decreasing galaxy luminosity (see Fig.15), implying, even in the innermost regions, the presence of a dark component whose importance increases with decreasing luminosity. We fit this  $M/L-L$  relationship by modelling the mass of these galaxies with (i) a luminous mass component with  $M_\star = 5 L_V$  (as Mateo 1997) and (ii) a dark halo with profile given by eq.(5). Then, also these objects have a ‘spiral’ dark-to-luminous mass ratio. For  $r \ll r_e$  the mass profile of a Hernquist spheroid is very similar to that of a ‘sphericized’ Freeman disk, for which we can write  $L(x) = L_V [1 - (1 + 3.2x)e^{-3.2x}]$ . We obtain the model’s central  $M/L$  ratios from  $\lim_{x \rightarrow 0} [M_h(x) + M_\star(x)]/L(x)$  (see Fig.15). The agreement between the model and observations is striking, although (a) we have extrapolated luminosities and radial distances by a factor of  $\sim 100$  and (b) the model has no free parameter. As a consequence, we find  $M_h \propto L_V^{1/4}$ , which is indistinguishable from Mateo’s best fit,  $M_h \sim 2 \times 10^7 M_\odot$  independent of

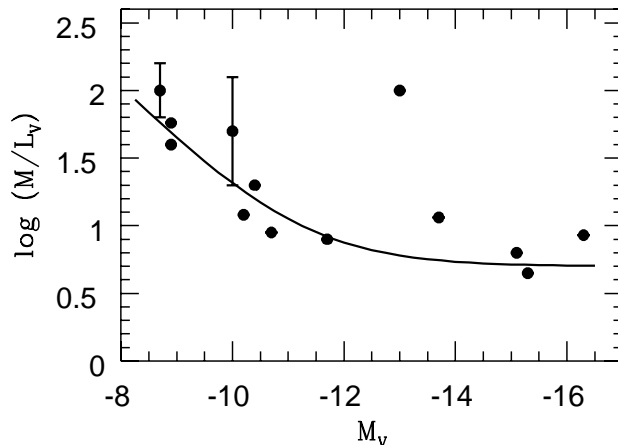


Figure 15. The  $M/L$  ratios of dIrr's: the observational data (from Mateo 1997: circles) vs. our prediction from the 'spiral' mass model (line)

luminosity, and in qualitative agreement with pioneering studies of the dSph Fundamental Plane (Ferguson & Binggeli 1994).

The present data, referring to central regions, do not allow one to derive the run of  $a$  with luminosity and then evaluate the central halo density. Taking a tentative value for  $a \sim R_c$ , the King radius, yields central overdensities  $10^6 - 10^7$  which make these galaxies among the densest of the Universe, as is obvious from the fact that these tiny galaxies withstand, at a distance of few tens of kpc, the gravitational tides of large galaxies like M31 and our own (Gallagher et al. 1997).

## 7. The structure of dark halos

In the previous section we have shown that the structure of dark halos around galaxies has a universal character: a specific functional form, with two mass dependent-parameters, describes the density distribution of dark halos at any radius, in all galaxies of every Hubble type. Here, we discuss the basic properties of such a DM distribution and the relevant aspects of the interplay between dark and luminous matter. These can be divided into (a) universal properties, that is, not depending on Hubble type, and (b) morphological properties which do depend on Hubble type.

### 7.1. Universal properties

From the kinematics of a very large number of disk and spheroidal systems, there unquestionably emerges a one-to-one relation between a luminous galaxy and a massive dark halo. This is the rule: a hypothetical galaxy found with no dark halo should be considered as a peculiar exception. Galaxies lie within large self-gravitating dark halos: more specifically, a disk/spheroid of size  $R_{opt}$

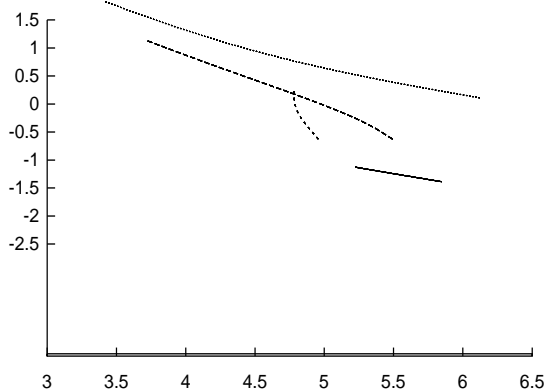


Figure 16. Luminous-to-dark mass ratio vs. halo central density diagram. Always, higher DM fractions correspond to higher densities. (Dotted curve: E's; long-dashed curve: spirals; short-dashed curve: LSBs; solid curve: dIrr's.)

and mass  $M_*$ , should be actually seen as embedded in a dark halo of radius  $\sim R_{200} \sim 15 R_{opt}$  and mass  $M_{200} = 3 \times 10^{12} (\frac{M_*}{2 \times 10^{11} M_\odot})^{0.4} M_\odot$ .

▷ The luminous matter, not surprisingly considering the dissipational collapse it has experienced, is more concentrated, by a factor  $\sim 10 - 15$ , than the dark matter. This explains why the former nearly always dominates the inner regions of galaxies, where the luminous-to-dark matter density ratio is always  $\gg 10^4 \Omega_b \beta \gg 1$ . From the galaxy center out to  $R_{opt}$ , the fraction of DM goes from 0% up to 30% – 70%. Thus, all across the region where the baryonic matter resides, the dark and luminous components are well mixed, except in very-low-luminosity galaxies, dominated by the dark matter at all radii. Thus, two common (and competing) ideas, according to which either *i*) dark matter is the main component inside  $R_{opt}$  or *ii*) dark matter is important only where the stellar distribution ends, are both ruled out by observational evidence. In the same way, the very concept of mass-to-light ratio retains its physical meaning only if the radius at which a value is derived is specified.

▷ DM halos have core radii, i.e. regions of width  $\sim R_{opt}$ , where the DM density remains approximately constant. Let us stress that the core is apparent in every galaxy of every Hubble type, not only in dIrr's (see Moore 1994). Actually, this region is larger in larger galaxies, both in physical and in normalized units. The existence of core radii makes the central density of a DM halo a well-defined, physically meaningful quantity, and it implies that DM halos, even though arising from scale-free perturbations, do actually develop a scale, related with the half-light scale. The well proven existence of core radii, furthermore, rules out all halo models with a prominent central cusp or with a hollow core.

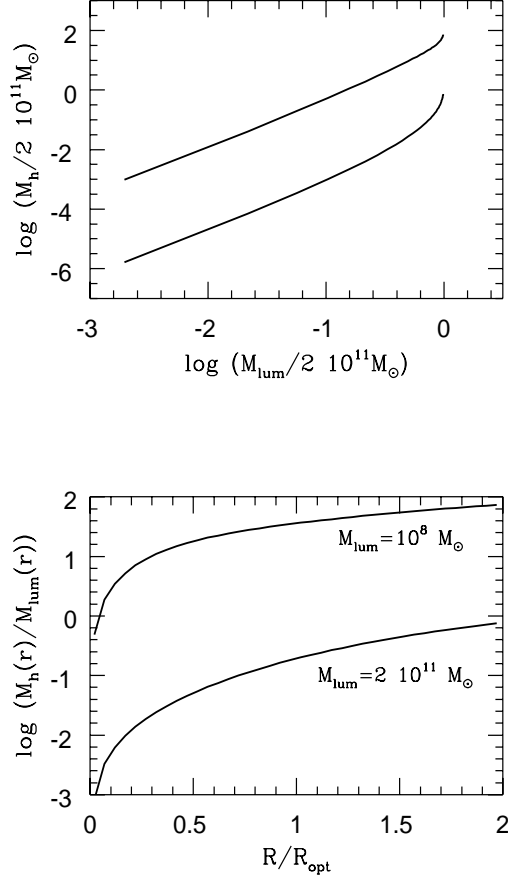


Figure 17. The dark-to-luminous mass ratio for high and low values of the stellar mass ( $M_\star = 2 \times 10^{11} M_\odot$  and  $M_\star = 10^8 M_\odot$ , respectively) as a function of normalized radius (*bottom*); within a specified radius, DM mass vs. luminous mass (*top*).

▷ The DM central densities range through about 3 orders of magnitude, inversely correlated with galaxy luminosity (see Fig.16), consistently with hierarchical scenarios of galaxy formation in which smaller objects form first.

▷ Proto-galaxies are likely to start their collapse with the same baryon fraction  $\Omega_b$ . However, in present-day galaxies this quantity strongly depends on the galaxy luminosity (halo mass), ranging from  $\sim \Omega_b$  at high masses  $\gtrsim 10^{11} M_\odot$ , to  $10^{-4} \Omega_b$  at the lowest mass  $\sim 10^8 M_\odot$ . The efficiency of retaining the primordial gas and transforming it in stars is then a strong function of the depth of the (halo) potential well.

▷ The range in luminosity among galaxies,  $> 3$  orders of magnitude, is much wider than that of halo masses, which spans through  $< 2$  orders of magnitude. This implies that the global mass-to-light ratios of galaxies decrease with increasing halo mass as  $\frac{M_{200}}{L} \propto M_{200}^{-1}$ . According to the above, considering all

galaxies as having the same total mass, is not as bad as assuming that their masses and luminosities are directly proportional. In this light, the persistent habit in many cosmological studies of assuming  $M_{\text{halo}}/L = \text{const}$  should be avoided, if possible.

▷ In every galaxy and at any radius, the distributions of dark and luminous matter are coupled: the luminous matter knows where the dark matter is distributed and viceversa. The coupling is universal, in that it is essentially independent of the Hubble type of the galaxy. At a (normalized) radius  $x = R/R_{\text{opt}}$  the mass ratio takes the form:

$$\frac{M_h(x)}{M_\star(x)} = 0.16 \left( \frac{M_\star}{2 \times 10^{11} M_\odot} \right)^{3/4} \left[ 1 + 3.4 \left( \frac{M_\star}{2 \times 10^{11} M_\odot} \right)^{1/3} \right] \times \frac{x^2}{\left[ x^2 + 3.4 \left( \frac{M_\star}{2 \times 10^{11} M_\odot} \right)^{1/3} \right] \left[ 1 - (1 + 3.2x) e^{-3.2x} \right]}. \quad (26)$$

In Fig.(17) we show the radial dependence of the dark-to-luminous mass ratio for the highest and lowest stellar masses,  $2 \times 10^{11} M_\odot$  and  $10^8 M_\odot$ , and the dark matter inside a fixed radius  $R$  as a function of the luminous matter inside that radius. The dark-luminous coupling can be quantified by noting that, where the luminous mass is located ( $R \lesssim 2 R_{\text{opt}}$ ), over five orders of magnitude in mass and independently of the total stellar (or halo) mass,  $M_\star \propto M_h^{2/3}$ ; this relationship breaks down where the stellar distribution converges. This interplay is the imprint of the late stages of the process of galaxy formation and rules out the concept of “cosmic conspiracy”. On the theoretical side, we emphasize that it is difficult to envisage how such a structural feature may arise in scenarios radically different from a (CDM-like) bottom-up.

## 7.2. Morphological dependence

While the universal behaviour of the mass distribution of dark halos relates to the cosmological properties of DM, any Hubble type dependence of the distribution of the luminous and dark matter characterizes the late processes of galaxy formation, such as transfer of angular momentum, the efficiency of the star formation and its feed-back on galaxy structure. Remarkably, a small number of structural quantities allow one to describe the gross features of the morphological/luminosity dependence of the DM distribution and of the interplay with the luminous matter. These are: the central DM density  $\rho_0$ , the core radius  $a$  (in units of  $R_{\text{opt}}$ ) and the luminous-to-dark mass ratio evaluated at the optical radius. For each Hubble Type, the above structural parameters are all functions of luminosity and then correlate among themselves. In Fig.(18) we show, for each Hubble type, the curves generated in the space  $\rho_0, a, \frac{M_h}{M_\star}|_{x=1}$  by the variation of luminosity. We note that:

◦ the DM structural parameters and the connection with the luminous matter show a strong continuity when passing from one Hubble Type to another. This happens despite the fact that both the distribution and the global properties of the luminous matter show strong morphological discontinuities;

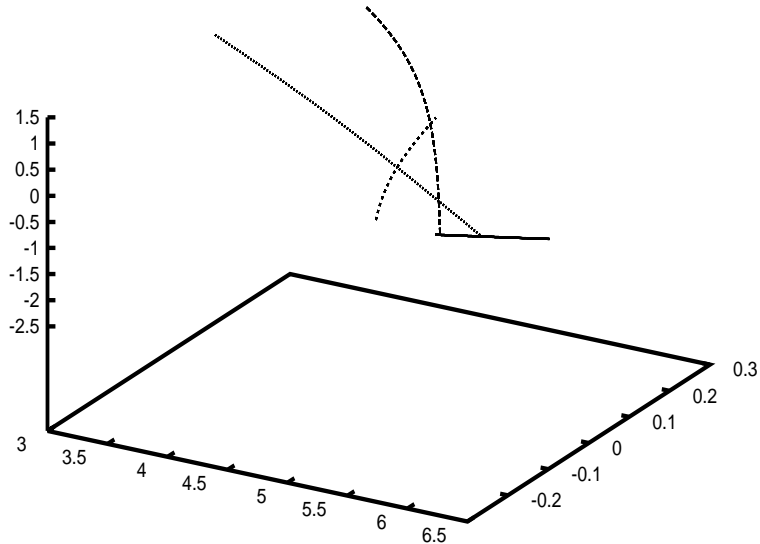


Figure 18. The loci populated by the families of galaxies in the luminous-to-dark mass ratio at  $R_{opt}$ , halo central density, and (halo core)-to-optical radius ratio space ( $z/x/y$ ). (From left to right, we encounter ellipticals, spirals and LSBs, and dIrr's.)

◦ dwarf galaxies, the densest galaxies in the Universe, are also completely dark-matter dominated: however, their low baryon content just smoothly continues downwards the dependence with galaxy mass followed by larger galaxies. As this continuity extends to all other structural properties, the tendency to theoretically investigate these objects separately from “normal” galaxies could be misleading;

◦ spirals show the largest range in dark-to-luminous mass ratios and central densities, indicating that the occurrence of this morphological type is independent of the structure/evolution parameters considered here. This is probably because the main factor responsible for the formation of disk systems, i.e. the content of angular momentum, is likely to be independent of halo mass;

◦ LSB galaxies are significantly less dense than normal spirals. As this is the case for both the dark and luminous components, the fractional amount of dark matter is not affected. This ratio, as well as the size of the halo core radius, depends on galaxy luminosity as in HSB spirals. LSBs, instead, are clearly distinguished by having both lower  $\rho_0$  and lower stellar mass-to-light ratios. This suggests that the differentiation between HSB and LSB galaxies is due to different initial conditions (e.g., content of angular momentum, epoch of formation) rather than being developed during the late stages of formation;

◦ ellipticals, considered as luminous spheroids, are well characterized objects, evidently very different from disk systems. However, in the structural parameter space, E and S galaxies are contiguous, the main difference being that the former are more concentrated in both the dark and luminous components. Combined with the evidence that the dark halos of ellipticals have smaller core radii (both

in normalized and in physical units), this morphological property may be due to a deeper baryonic infall in the halo potential well.

**Acknowledgements.** We thank Erwin de Blok for sending his LSB rotation curve data. We also thank Lynn Matthews for communicating data prior to publication. We acknowledge John Miller for carefully reading the manuscript. Finally, special thanks are due to all the participants to the Sesto DM1996 conference, without whom this paper would not have been possible.

## References

- Armandroff, T. E., Olszewski, E. W., & Pryor, C. 1995, *AJ*, 110, 2131  
Ashman, K.M. 1992, *PASP*, 104, 1109  
Ashman, K.M., Salucci, P., & Persic, M. 1993, *MNRAS*, 260, 610  
Bender, R., Burstein, D., & Faber, S.M. 1992, 399, 462  
Bertin, G., Saglia, R.P., & Stiavelli, M. 1992, *ApJ*, 384, 423  
Bertola, F., Pizzella, A., Persic, M., & Salucci, P. 1993, *ApJ*, 416, L45  
Bosma, A. 1981, *AJ*, 86, 1825  
Broeils, A.H. 1992, PhD thesis, Groningen U.  
Broeils, A.H., & Courteau, S. 1997, this volume  
Bruzual, A.G. 1983, *ApJ*, 273, 105  
Caon, N., Capaccioli, M., & D’Onofrio M. 1993, *MNRAS*, 265, 1013  
Carignan, C., & Freeman, K.C. 1988, *ApJ*, 332, L33  
Carollo, C.M., & Danziger, I.J. 1994, *MNRAS*, 270, 523  
Carollo, C.M., de Zeeuw, P.T., van der Marel, R.P., Danziger, I.J., Qian, E.E. 1995, *ApJ*, 441, L25  
Casertano, S., & van Gorkom, J.H. 1991, *AJ*, 101, 1231  
Charlton, J.C., & Salpeter, E.E. 1991, *ApJ*, 375, 517  
Côté, S. 1995, PhD thesis, Australian National University  
Côté, S., Freeman, K., & Carignan, C. 1997, this volume  
Danziger, I.J. 1997, this volume  
de Blok, W.J.G., McGaugh, S.S., & van der Hulst, J.M. 1996, *MNRAS*, 283, 18  
de Blok, W.J.G., & McGaugh, S.S. 1997, this volume  
de Vaucouleurs, G. 1948, *Ann. D’Astroph.*, 11, 247  
Disney, M., & Phillips, S. 1983, *MNRAS*, 205, 1253  
Djorgovski, S., & Davis, M. 1987, *ApJ*, 313, 59  
Djorgovski, S., & Santiago, B.X. 1993, in “Structure, Dynamics, and Chemical Evolution of Early-Type Galaxies”, ed. I.J.Danziger et al. (ESO Conf.Publ., 45), 59  
Dressler, A., et al. 1987, *ApJ*, 313, 42  
Driver, S.P., Phillips, S., Davies, J.I., Morgan, I., & Disney, M.J. 1994, *MNRAS*, 266, 155  
Faber, S.M., & Lin, D.M.C. 1983, *ApJ*, 266, L17



- Fabricant, D., & Gorenstein, P. 1983, ApJ, 267, 535
- Ferguson, H.C., & Binggeli, B. 1994, A&AR, 6, 67
- Freeman, K.C. 1970, ApJ, 160, 811
- Frenk, C.S., White, S.D.M., Davis, M., & Efstathiou, G. 1988, ApJ, 327, 507
- Gallagher, J.S., Han, M., & Wyse, R.F.G. 1997, this volume
- Graham, A., & Colless, M. 1997, this volume
- Hargreaves, J. C., Gilmore, G., Irwin, M. J., & Carter, D. 1994, MNRAS, 271, 693
- Hargreaves, J. C., Gilmore, G., Irwin, M. J., & Carter, D. 1996, MNRAS, 282, 305
- Hendry, M., Persic, M., & Salucci, P. 1997, this volume
- Ibata, R. A., Wyse, R. F. G., Gilmore, G., Irwin, M. J., & Suntzeff, N. B. 1997, AJ, in press [astro-ph/9612025]
- Kormendy, J. 1988, in “Origin, Structure, and Evolution of Galaxies”, ed. L.Z.Fang (World Scientific), 252
- Lanzoni, B. 1994, Laurea thesis, Bologna U.
- Mateo, M. 1994, ESO/OHP Workshop, ed. G.Meylan & P.Prugniel, 309
- Mateo, M. 1997, in “The Nature of Elliptical Galaxies”, ed. M.Arnaboldi, G.S.DaCosta, & P.Saha, in press
- Matthews, L.D., Gallagher, J.S., & van Driel W. 1997, this volume
- Morshidi, Z., Davies, J.I., & Smith, R. 1997, this volume
- Moore, B. 1994, Nature, 370, 629
- McGaugh, S.S., & Bothun, G.D. 1994, AJ, 107, 530
- Navarro, J.F., Frenk, C.S., & White S.D.M. 1996, ApJ, 462, 563
- Persic, M., & Salucci, P. 1988, MNRAS, 234, 131
- Persic, M., & Salucci, P. 1990, MNRAS, 245, 577
- Persic, M., & Salucci, P. 1991, ApJ, 368, 60
- Persic, M., & Salucci, P. 1995, ApJS, 99, 501
- Persic, M., Salucci, P., & Stel, F. 1996, MNRAS, 281, 27
- Pryor, C. in “Morphological and Physical Classification of Galaxies”, ed. G.Longo, M.Capaccioli, & G.Busarello (Dordrecht: Kluwer), 163
- Puche D., & Carignan, C. 1991 ApJ, 378, 487
- Queloz, D., Dubath, P., & Pasquini, L. 1995, A& A, 300, 31
- Renzini, A., & Ciotti, L. 1993, ApJ, 416, L49
- Rhee, M.-H. 1996, PhD thesis, Groningen U.
- Rhee, M.-H., & van Albada, T.S. 1997, preprint
- Richstone, D.O., & Tremaine, S. 1986, AJ, 92, 72
- Rix, H.-W., de Zeeuw, P.T., Carollo, C.M., Cretton, N., & van der Marel, R.P. 1997, astro-ph/9702126
- Romanishin, W., Strom, S.E., & Strom, K.M. 1982, ApJ, 258, 77
- Rubin, V.C., Ford, W.K., & Thonnard, N. 1980, ApJ, 238, 471
- Saglia, R.P., Bender, R., Gerhard, O.E., & Jeske, G. 1997, this volume

Saglia, R.P., Bernardi, M., Bertola, F., Pizzella, A., Buson, L.M., De Bruyne, V., Dejonghe, H., & Zeilinger, W.W. 1997, this volume  
Salucci, P., & Frenk, C.S. 1989, MNRAS, 237, 247  
Schombert, J.M., Bothun, G.D., Schneider, S.E., & McGaugh, S.S 1992, AJ, 103, 1107  
Sincotte, V., & Carignan, C. 1997, AJ, 113, 690  
Sprayberry, D., Impey, C.D., Irwin, M.J., McMahon, R.G., & Bothun, G.D. 1993, ApJ, 417, 114  
Swaters, R. 1997, this volume  
Tinsley, B.M. 1981, MNRAS, 194, 63  
van der Marel, R.P. 1991, MNRAS, 253, 710  
van der Marel, R.P. 1994, PhD thesis, Leiden U.  
van der Marel, R.P., & Franx, M. 1993, ApJ, 407, 525  
Vogt, S., Mateo, M., Olszewski, E. W., & Keane, M. J. 1995, AJ, 109, 151  
Zaritsky, D. 1997, this volume  
Zaritsky, D., Smith, R., Frenk, C., & White, S.D.M. 1993, ApJ, 405, 464

## 8. Appendix

In this paper we have used data coming from many different sources. In detail:

□ *Spiral Galaxies*. See references quoted in PSS96.

□ *LSB Galaxies*. We have used all the objects in the de Blok et al. (1996) sample, except for: F567-2, F577-V1, F579-V1 (asymmetric velocity arms), F571-V2 (optical scalelength missing), and F564-V3 (rotation curve missing).

□ *Elliptical Galaxies*. The sources are:

N 720: Buote & Canizares 1994, ApJ, 427, 86;

N1052, N2974, N4278, N5077, N7097, I2006:

Bertola et al. 1993, ApJ, 416, L45 (and refs. therein);

N 1453: Pizzella 1997, private communication;

N 1399: Ikebe et al. 1996, Nature, 379, 427;

N 4697: Dejonghe et al. 1996, A&A, 306, 363;

N 5128: Hui et al. 1995, ApJ, 449, 592;

N 6703: Saglia et al. 1997, this volume.

□ *Dwarf Irregular Galaxies*. The sources are:

DDO 154: Carignan & Freeman 1988, ApJ, 332, L33;

UGC 442, E381-G20, DDO 161, E444-G84: Côté 1997, this volume;

DDO 170: Lake et al. 1990, AJ, 99, 547;

I3522, U7906: Skillman et al. 1987, A&A, 185, 61;

DDO 175: Skillman et al. 1988, A&A, 198, 33;

UGC 12732, DDO 9: Swaters 1997, this volume.

□ *Dwarf Spheroidal Galaxies*. The sources are Mateo (1997) and references therein.